Packing-limited growth

Peter Sheridan Dodds[1,*] and Joshua S. Weitz[2,3,†]
[1]*Columbia Earth Institute, Columbia University, New York, New York 10027*
[2]*Department of Earth, Atmospheric and Planetary Sciences, Massachusetts Institute of Technology, Cambridge, Massachusetts 02139*
[3]*Department of Physics, Massachusetts Institute of Technology, Cambridge, Massachusetts 02139*
(Received 31 December 2001; published 6 May 2002)

We consider growing spheres seeded by random injection in time and space. Growth stops when two spheres meet leading eventually to a jammed state. We study the statistics of growth limited by packing theoretically in d dimensions and via simulation in $d=2$, 3, and 4. We show how a broad class of such models exhibit distributions of sphere radii with a universal exponent. We construct a scaling theory that relates the fractal structure of these models to the decay of their pore space, a theory that we confirm via numerical simulations. The scaling theory also predicts an upper bound for the universal exponent and is in exact agreement with numerical results for $d=4$.

DOI: 10.1103/PhysRevE.65.056108 PACS number(s): 64.60.−i, 87.23.Cc, 05.45.−a, 81.10.Aj

I. INTRODUCTION

The dynamic packing of objects is an often overlooked variation on the theme of static packing. Given a mechanism for the creation, growth, movement, and interaction of like objects in a given dimension, what structures result? Here, we find universal features of a simple yet broad class of such mechanisms falling under the rubric ''packing-limited growth'' (PLG). A PLG mechanism entails objects being seeded randomly, growing according to a rule that may be specific to each object, and stopping when a part of their boundary hits that of another object. A motivating physical example of this kind of pattern formation may be found in the competition between tree crowns in dense forests [1,2], the structure of porous media [3–5], and the generalized problem of dense packings [6].

A simple model of PLG has previously been studied by Andrienko, Brilliantov, and Krapivsky [7,8] (the ABK model). In their setting, spheres are seeded randomly in space and time. A sphere's radius increases linearly with time, halting when another sphere is touched. This model is amenable to an approximate analysis for $d>1$ [8] and has an exact solution in $d=1$. In this present work, we are interested in the limiting distribution of radii, $N(r)$. For PLG models, we expect $N(r)\propto r^{-\alpha}$ for small r. Note that the fractal dimension D of the set comprising all sphere centers, which is often measured instead of α, is related to α as $D=\alpha-1$ [9]. In $d=1$, the exact solution gives $\alpha=1$, which corresponds to $D=0$ (meaning the number of centers diverges logarithmically) [8]. For $d=2$, Andrienko *et al.* [7] report that $D\simeq 1.75$ and hence $\alpha\simeq 2.75$ based on numerical evidence. Elsewhere, the same authors [8] determine numerically that $\alpha\simeq 2.53$.

We claim that the actual value of α is essentially independent of the specifics of the growth dynamics. To see why, we examine a related $d=2$ random packing model due to Manna [9]. The packing process begins in a finite-sized volume (or alternatively with an initial population of fixed radius disks). New disks are added one at a time by randomly choosing a point in the packing's pore space and centering there the largest possible nonoverlapping disk. Manna finds $\alpha\simeq 2.62$ and $\alpha\simeq 2.64$ for two example packings.

We refer to the Manna model as ''random Apollonian packing'' (RAP) since it may be seen as a variation of the well known Apollonian packing [10]. For the $d=2$ version of the latter, pore spaces are always formed by three disks each touching the other two and disks are added so as to fill the pore space fully (i.e., the inserted disk touches all three of its surrounding neighbors). Numerics give $\alpha\simeq 2.31$ for Apollonian packing in agreement with analytically derived bounds [11]. Aste [12] has shown for static polydisperse packings that are space filling, Apollonian packing provides the lowest bound on α while the upper bound is $\alpha=d+1$.

There are two important observations to make here. First, as noted by Brilliantov *et al.* [8], the RAP model is the ABK model in the case of infinitely fast growth: as soon as a sphere is nucleated, it instantaneously expands to hit the nearest sphere boundary. Second, for general PLG models, pore spaces evidently increase in number and decrease in size with time. This means that the likelihood of two spheres nucleating in the same pore space also decreases. Eventually the mechanism of the RAP model must take over, and all collisions will be between a growing sphere in a pore space and a ''stuck'' sphere forming part of the pore space boundary. Thus, the RAP model is not just a curious end point of the ABK model but, in fact, entails the sole mechanism describing how small radius spheres pack. We suggest then that measurements of α in the ABK model should coincide with revised estimates from simulations of the RAP model. In the remainder of the paper, we describe a general class of PLG models for which α is invariant, provide a simple solution for the $d=1$ problem, develop a scaling theory that describes how the radii distribution and volume of pore space evolve with time, and provide results from extensive numerical simulations.

II. GENERAL MODEL OF PACKING-LIMITED GROWTH

For our general conception of PLG we take d-dimensional spheres growing in a volume V. Spheres are nucleated ran-

*Electronic address: dodds@ldeo.columbia.edu
†Electronic address: jsweitz@segovia.mit.edu

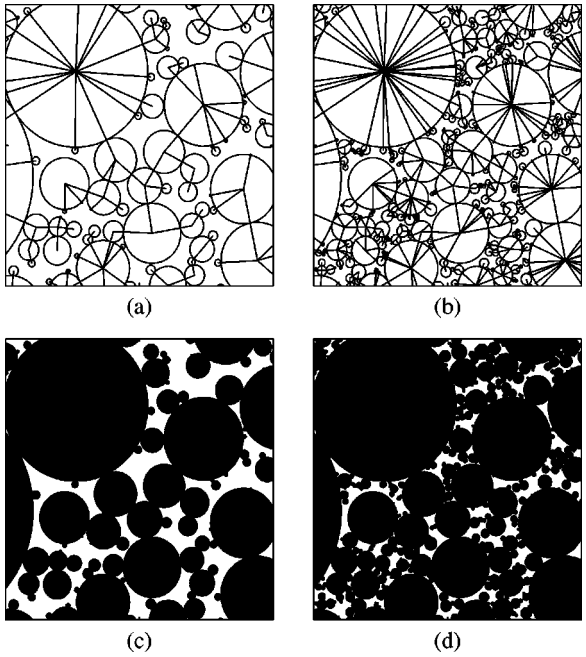

FIG. 1. The dynamics and limiting states of PLG models.In (a) and (b), collisions between centers are marked with lines while in (c) and (d), the regions occupied by spheres are black and the pore space is left white. All four pictures come from the same simulation, (a) and (c) depict the condition of a subsection of a system packed with 500 spheres, (b) and (d) depict the same subsection after 2000 spheres have been packed.

domly in space at a rate κ per unit volume surviving only if they are injected into the unoccupied pore space. All spheres stop growth upon contact with a neighboring sphere. Figure 1 provides a visual context for the dynamics explained below. The ith sphere, which is initiated at t_i, grows at a rate $G_i(t-t_i)$ giving the radius $r_i(t)$ as

$$r_i(t)=\int_0^{t-t_i} G_i(u)\,\mathrm{d}u, \tag{1}$$

for $t \geqslant t_i$. We assume the weak requirement that each sphere grows in a strict monotonic fashion, i.e., for each i, $G_i(t-t_i) \geqslant \epsilon > 0$. The model is thus one of arbitrary individual growth limited solely by packing. The dynamics continue in the above fashion until the volume V is completely filled and a final jammed state is reached.

Consider an individual pore Γ of diameter λ (i.e., the maximum separation of two boundary points that can be joined by a line contained entirely within the pore). The rate ν at which spheres nucleate in Γ (excluding growth for the moment) is given by

$$\nu \simeq \kappa V_d \lambda^d, \tag{2}$$

where V_d is the volume of d-dimensional sphere of unit radius. The typical time τ between nucleations in Γ is, therefore,

$$\tau = 1/\nu \simeq \kappa^{-1} V_d^{-1} \lambda^{-d}. \tag{3}$$

On the other hand, if sphere i nucleates in Γ, it will jam in a time τ_{jam} that can be no greater than the time it takes for its radius to reach $\lambda/2$. Together with the assumption that $G_i(t-t_i) \geqslant \epsilon > 0$, this gives

$$\tau_{\mathrm{jam}} \lesssim \lambda/2\epsilon. \tag{4}$$

So when $\tau_{\mathrm{jam}} \ll \tau$, i.e., when

$$V_d \lambda^{d+1} \kappa/2\epsilon \ll 1, \tag{5}$$

we expect the packing mechanism to be the same as the RAP model—all spheres will be stopped by an existing stopped sphere and never by another moving sphere. Growth rate, therefore, becomes irrelevant as far as the final packing is concerned. From Eq. (5), we see that the general model reduces to the RAP model when the maximum pore size $\lambda_{\max}$ satisfies

$$\lambda_{\max} \ll (2\epsilon/V_d\kappa)^{1/(d+1)}. \tag{6}$$

Since $\lambda_{\max}$ steadily decreases with t (i.e., space fills up) this condition will always be eventually satisfied.

III. EXACT $d=1$ SOLUTION

As we have noted, the ABK model has been solved exactly in the $d=1$ case [8] with the outcome being $\alpha=1$. Here, we achieve the same result with a considerably simpler calculation. Since we have posited that α is a universal exponent for a general class of packing-limited growth models, we may choose the straightforward example of the $d=1$ RAP model. We take the unit interval $[0,1]$ as the initial vacant pore space. Spheres are now line segments and are limited either on the left or right as they are added with the points 0 and 1 providing initial boundaries. Thus, the unit interval is filled in from each end with the one solitary pore space diminishing in the middle. Writing the length of the nth line segment as l_n we have

$$l_n = z_{n-1}\left(1-\sum_{i=1}^{n-1} l_i\right), \tag{7}$$

where z_i is a random number uniformly distributed on the unit interval and $l_1=z_0$. In other words, each new line segment is a random fraction of the current pore space. Iteratively solving Eq. (7) gives

$$l_n = z_{n-1}\prod_{i=0}^{n-2}(1-z_i). \tag{8}$$

We can in principle find the distributions of the l_i but for our present purposes their means are sufficient and we have

$$\langle l_n \rangle = 2^{-n}. \tag{9}$$

We, therefore, expect the typical number of line segments with $l' \geqslant l = 2^{-n}$ to be

$$N(l' \geqslant l = 2^{-n}) = n = -\frac{\ln l}{\ln 2}. \tag{10}$$

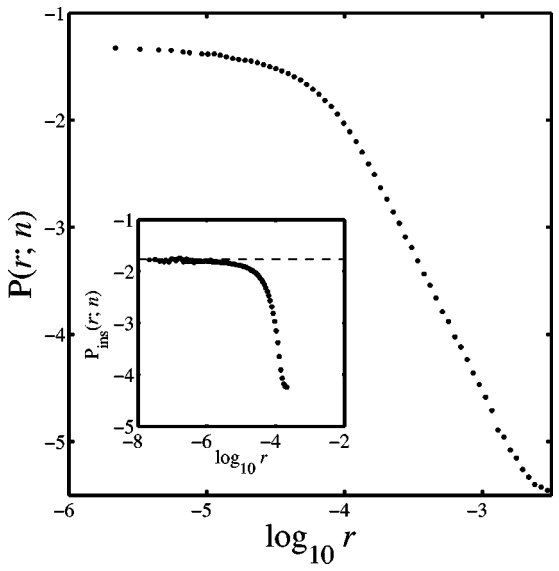

FIG. 2. $P(r;n)$ for a $d=2$ RAP simulation with $n=10^6$. The inset distribution is $P_{\rm ins}(r;n)$, which is obtained by simulating the RAP procedure for another 10^6 disks without actually inserting any of them into the pore space. The dashed line in the inset figure corresponds to the theoretical prediction $P_{\rm ins}(0;n)=S(n)/\Phi(n)$.

Since this is the cumulative frequency distribution, i.e., $N(l' \geqslant l)=\int_l^\infty N(l')\mathrm{d}l'$, we find the frequency distribution $N(l)$ must behave as

$$N(l) \simeq \frac{1}{\ln 2} l^{-1}, \tag{11}$$

yielding, as expected, $\alpha=1$.

IV. DESCRIPTION OF INSERTION PROBABILITY AND PORE SPACE VOLUME

We next investigate the form of $P_{\rm ins}(r;n)$, the probability distribution of the $(n+1)$th sphere's radius to be inserted into a packing. In addition, we characterize $P(r;n)$, the probability distribution of sphere radii after n spheres have been packed. Note that since we have shown that a general class of PLG models reduce to the RAP model, we now use the number of spheres n rather than time t to index our quantities.

We first note that the distribution $P(r;n)$ fills in from the right with increasing n. As the packing fills in space, the maximum pore size either decreases or does not change and so does the maximum size of any sphere that may be added. We write the radius of this largest sphere as r_c. We observe that to a first approximation, $P(r;n)$ above this cutoff scale r_c follows its limiting power law form while below the distribution it is essentially flat (see Fig. 2). For the purposes of estimation, we assume this form exactly as

$$P(r;n)=\begin{cases} \dfrac{\alpha-1}{\alpha} r_c^{-1} & \text{for } r<r_c \\ \dfrac{\alpha-1}{\alpha} r_c^{-1}\left(\dfrac{r}{r_c}\right)^{-\alpha} & \text{for } r \geqslant r_c. \end{cases} \tag{12}$$

The corresponding frequency distribution is $N(r;n) \propto P(r;n)$. Since the tail of $N(r;n)$ remains fixed as n increases, we can obtain the scaling of r_c with n. From Eq. (12), the tail of $N(r;n)$ behaves as

$$N(r;n)=\frac{\alpha-1}{\alpha} n r_c^{\alpha-1} r^{-\alpha}=k r^{-\alpha}, \tag{13}$$

for $r>r_c$. Since the prefactor k must be constant, we have

$$r_c=\left(\frac{\alpha-1}{\alpha k} n\right)^{-1/(\alpha-1)} \propto n^{-1/(\alpha-1)}. \tag{14}$$

The uniformity of $P(r;n)$ for $r<r_c$ closely relates to the form of $P_{\rm ins}(r;n)$. It is possible to write down an exact expression for $P_{\rm ins}(r;n)$, that is,

$$P_{\rm ins}(r;n)=\frac{\int dV \delta[D_n(\vec{x})-r]}{\int dV}, \tag{15}$$

where the integrals are over the pore space, and $D_n(\vec{x})$ is the distance from the point $\vec{x}$ to the closest pore space boundary after n spheres have been inserted. This integral may be solved exactly in the limit of very small radii,

$$\lim_{r\to 0} P_{\rm ins}(r;n)=\frac{S(n)}{\Phi(n)}, \tag{16}$$

where $S(n)$ and $\Phi(n)$ are the surface area and available pore space of the existing n packed spheres. This means that the region of pore space available for insertion of an infinitesimal sphere is proportional to the surface area of the extant packing. Assuming that this holds approximately for all spheres below the cutoff, the full distribution $P_{\rm ins}(r;n)$ may be modeled as a purely flat distribution,

$$P_{\rm ins}(r;n)=\begin{cases} r_c^{-1} & \text{for } r<r_c \\ 0 & \text{for } r \geqslant r_c. \end{cases} \tag{17}$$

Good agreement with this approximation is shown in the inset of Fig. 2. Comparing Eq. (16) with Eq. (17), we see that $r_c=\Phi(n)/S(n)$. We calculate $S(n)$ and $\Phi(n)$ using $N(r;n)$,

$$S(n)=\frac{k\alpha V_d}{\alpha-d} r_c^{-(\alpha-d)}, \tag{18}$$

and

$$\Phi(n)=\frac{k\alpha V_d}{(d+1)(d+1-\alpha)} r_c^{d+1-\alpha}, \tag{19}$$

where as before V_d is the volume of a unit radius sphere in d dimensions. Note that $S(n)\to\infty$ and $\Phi(n)\to 0$ as $n\to\infty$.

Using Eqs. (18) and (19), and the result $r_c=\Phi(n)/S(n)$, we find an estimate of α as

TABLE I. Scaling relations between exponents for various parameters valid for general packing-limited growth models: $P(r)$ is the probability distribution of radii, r_c is the radius of the typical largest sphere that may be inserted, $S(n)$ is the surface area of n packed spheres, and $\Phi(n)$ is the pore space volume. All exponents are given in terms of α and the dimension d.

Relation	Exponent
$P(r) \propto r^{-\alpha}$	α
$r_c(n) \propto n^{-\delta}$	$\delta = d+1-\alpha$
$S(n) \propto n^{\gamma}$	$\gamma = (\alpha-d)/(\alpha-1)$
$\Phi(n) \propto n^{-\beta}$	$\beta = (d+1-\alpha)/(\alpha-1)$

$$\hat{\alpha} = d + \frac{d+1}{d+2}. \tag{20}$$

In contrast, a modified calculation for the ABK model finds [8]

$$\alpha_{\mathrm{mf}} = 1 + d\left(1 + \exp\left[2 - \frac{2^{d+2}-2}{d+2}\right]\right). \tag{21}$$

Note that $\hat{\alpha}$ must be an upper bound on the true value of α for normal Apollonian packing. Furthermore, due to the nature of the approximations made in forming $P_{\mathrm{ins}}(r;n)$ and $P(r;n)$, $\hat{\alpha}$ is also an upper bound for the exponent of the RAP model. As we show in the following section when we consider our numerical results, both of these predictions of α appear to hold for certain (mutually exclusive) ranges of d.

Using Eqs. (14), (18), and (19), we are able to find the scalings of surface area and pore space volume with n,

$$S(n) \propto n^{-\gamma} \propto n^{(\alpha-d)/(\alpha-1)}, \tag{22}$$

and

$$\Phi(n) \propto n^{-\beta} \propto n^{-(d+1-\alpha)/(\alpha-1)}. \tag{23}$$

These relations provide us with further methods for determining α and for testing scaling relations between the iterative and structural nature of the packing. Equation (23), in particular, affords a more robust measurement rather than obtaining α directly from $P(r;n)$, and we employ this fact in our numerical investigations.

Note that for comparison between the current theory and that of ABK we must convert scaling predictions that depend on time to those that depend on sphere number. Specifically, the ABK theory predicts $\Phi(t) \propto t^{-A}$, where $A = \exp[2 - (2^{d+2}-2)/(d+2)]$. Because the ABK model can be seen as a RAP model with infinite growth velocity, the time between events is inversely proportional to the pore space available (given a uniform rate for attempted nucleation κ). So the result for the decay of pore space from ABK may be rewritten as $\Phi_{ABK}(n) \propto n^{-\beta'}$, where

$$t_n = \frac{1}{\kappa} \sum_{i=1}^{n} \frac{1}{\Phi_{ABK}(i)}. \tag{24}$$

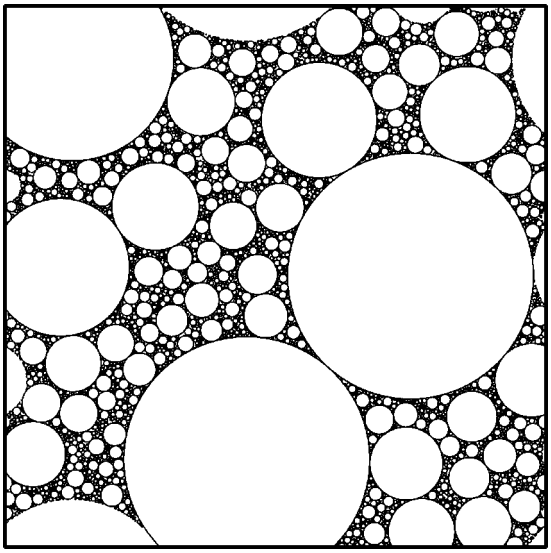

FIG. 3. A random Apollonian packing initially seeded with two circles after 10^4 circles have been placed. The density of the system is $\rho \simeq 0.94$.

This implies that $t_n \propto n^{1+\beta'}$. So if ABK predicts $\Phi(t) \propto t^{-A}$, this is equivalent to writing $\Phi_{ABK}(n) \propto n^{-A(1+\beta')}$. Equating the two forms leads to the conclusion that

$$\beta' = \frac{A}{1-A}. \tag{25}$$

This will be useful in the following section when the scaling of pore space decay is examined. Finally, key scaling relations are summarized in Table I.

V. NUMERICAL RESULTS

The numerical procedure for all variants of PLG schemes obey the same basic algorithm. Spheres are seeded according to a Poisson distribution, with rate κ and only grow within the pore space. Once injected, spheres grow according to model rules (linear velocity, heterogeneous, exponential, etc.) until they collide and are jammed. In the case of the RAP model, only one sphere is allowed to nucleate and expand at any given point in the simulation. Using this event driven procedure we are able to calculate limiting states and

TABLE II. Simulation details for four different PLG models. κ is the sphere nucleation rate per unit volume, $G_i(t-t_i)$ is the growth rate of the ith sphere, which is nucleated at time t_i, N_{s} is the number of simulations, N_{tot} is the total number of spheres placed, and ρ is the approximate limiting density of each simulation. The sphere radii distributions for these models are shown in Fig. 4.

	RAP	Heterogeneous	Exponential	Linear
κ	n/a	10	10	10^{-5}
$G_i(t-t_i)$	∞	0.2–2.0	e^{t-t_i}	0.2
N_{s}	50	48	10	1
N_{tot}	2.5×10^6	2.3×10^6	5.4×10^5	3.4×10^5
ρ	0.97	0.96	0.91	0.97

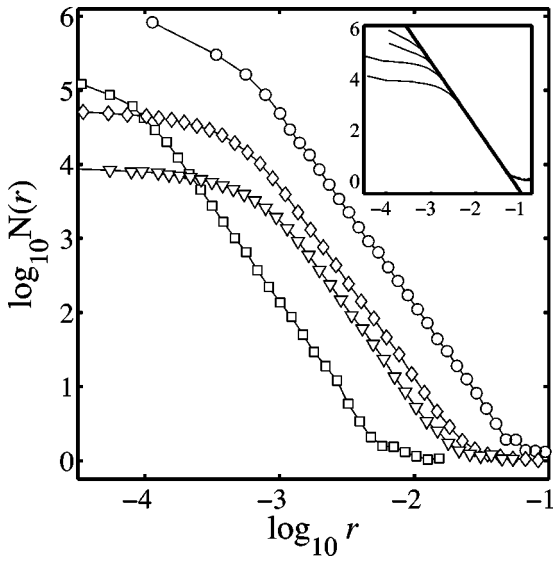

FIG. 4. The form of $N(r)$ for four models: random Apollonian packing (circles), heterogeneous linear growth rates (diamonds), exponential growth rates (triangles), and linear growth rates (squares). Simulation details are contained in the text. The inset double-logarithmic plot shows $N(r)$ vs r for each model shifted horizontally for the purpose of illustration. The slope of the solid straight line indicates the $d=2$ universal exponent $\alpha \simeq 2.56$ (see Table III).

determine improved estimates of the universal value of α for $d=2$, 3, and 4. All packings are simulated on a unit hypercube with periodic boundary conditions. Figure 3 shows an example packing using the RAP model in $d=2$. It is clear that the number of spheres will increase without bound and that the pore space ultimately vanishes. The associations with the Apollonian case are visually evident.

To demonstrate the universality of α, we consider four different PLG models in $d=2$ with a variety of initial conditions, the details of which are given in Table II. The frequency distribution $N(r)$ for these four PLG models is shown in Fig. 4. The main plot shows the distributions recentered using their respective means. The recentered distributions are indistinguishable to the eye clearly indicating that the specifics of the growth mechanisms are irrelevant and that the exponent α is a universal one.

The scaling theory developed in the preceding section relates the structure of a packing (its fractal dimension) to the change of basic elements (critical radius, surface area, volume, etc.) as a function of iteration. In order to test the scaling theory, as well as the specific prediction $\hat{\alpha}=d+(d+1)/(d+2)$ in higher dimensions, we now examine iterative and structural scalings of the RAP model in $d=2$, 3, and 4.

TABLE III. Estimates of α using various numerical methods and comparisons to theory. All numerical results are from simulations containing 5×10^6 spheres. Parentheses indicate 95% confidence intervals on the last digit.

	$d=2$	$d=3$	$d=4$
$\Phi(n)$	2.564(1)	3.733(2)	4.833(2)
$\Phi(r)$	2.58	3.73	4.83
$S(r)$	2.55	3.74	4.86
$N(r)$	2.53	3.70	4.79
$\hat{\alpha}=d+[(d+1)/(d+2)]$	2.75	3.8	4.83333
ABK theory	2.55374	3.94505	4.99904

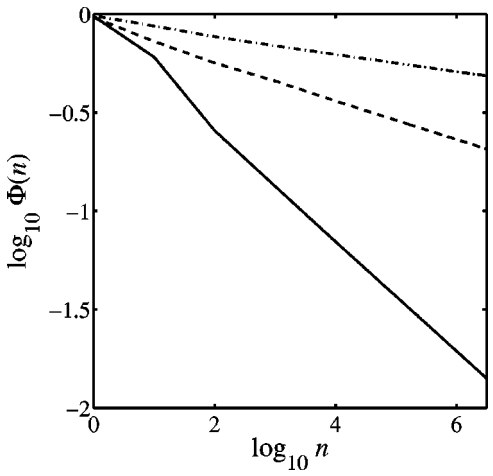

FIG. 5. The decay of pore space volume $\Phi(n)$ in $d=2$, 3, and 4 correspond to the solid, dashed, and dot-dashed lines, respectively. The fits to the power law decays are summarized in Table IV.

We estimate α using a variety of means and the results are summarized in Table III. The agreement between the predicted value of α calculated using $\Phi(n)$ and that calculated directly from the geometry of the packing provides further proof that the scaling theory outlined in the preceding section is valid, regardless of the specific value of α. The current theory appears to improve with increasing dimension, whereas the approximate theory of ABK only holds in $d=2$.

Both the current theory and that of ABK predict the scaling of pore space as a function of iteration or time. Evaluating the pore space decay $\Phi(n)$ in $d=2$ suggests that the agreement with ABK is most likely coincidental. As evidenced by the data in Fig. 5 we are able to establish 95% confidence intervals that exclude the predictions of ABK in $d=2$. This is not altogether surprising as ABK is an approximate theory describing the collision of moving spheres whereas in the RAP procedure all collisions are between a sphere and the presently jammed state. In higher dimensions, the theory of ABK fails, and the current theory becomes increasingly appropriate, falling within the numerically de-

TABLE IV. The predicted exponent for the decline of volume fraction $\Phi(n)\propto n^{-\beta}$. The numerical estimates of β are taken from simulations containing 5×10^6 spheres. The decay of pore space as a function of iteration can be seen in Fig. 5. Parentheses indicate error on estimation of the last digit.

	$d=2$	$d=3$	$d=4$
β	0.278(1)	0.0975(2)	0.0434(2)
Current theory (23)	0.1429	0.07143	0.04348
ABK theory (25)	0.2872	0.01832	2.404×10^{-4}

fined confidence intervals for β in $d=4$. The results are summarized in Table IV.

VI. CONCLUSION

The iterative nature of the random Apollonian packing model and its simple prescription for packing spheres suggests that at sufficiently small scales, the structure of packing-limited growth models is essentially unaffected by initial conditions or dynamics. The scaling of pore space, surface area, number, and critical radius r_c are all interrelated and can be expressed in terms of simple power laws using only the dimension d and the exponent α. Extensive numeric simulations demonstrate the validity of the predicted upper bound $\hat{\alpha}$. Although $\hat{\alpha}$ appears to be an overestimate of the actual value of α in $d=2$ and $d=3$, it agrees with simulations in $d=4$, and presumably beyond. A refined approximation of the insertion probability $P_{\mathrm{ins}}(r;n)$ seems to be the best approach to improve the estimate of α. The applicability of predictions of the present model and its relevance to physical and biological problems may lie in the process of balancing the idea of packing-limited growth with other dynamical possibilities such as aggregation, competition, and death.

ACKNOWLEDGMENT

This work was supported in part by the NSF through Grant No. EAR-9706220.

[1] H. S. Horn, *The Adaptive Geometry of Trees* (Princeton University Press, Princeton, NJ, 1971).
[2] K. Takahashi, Ann. Bot. (London) **77**, 159 (1996).
[3] D. Turcotte, *Fractals and Chaos in Geology and Geophysics*, 2nd ed. (Cambridge University Press, New York, NY, 1997).
[4] S.C. van der Marck, Phys. Rev. Lett. **77**, 1785 (1995).
[5] C. Hecht, Pure Appl. Geophys. **157**, 487 (2000).
[6] J. Conway and N. Sloane, *Sphere Packings, Lattices and Groups*, 3rd ed. (Springer-Verlag, New York, 1999).
[7] Y.A. Andrienko, N.V. Brilliantov, and P.L. Krapivsky, J. Stat. Phys. **75**, 507 (1994).
[8] N.V. Brilliantov, P.L. Krapivsky, and Y.A. Andrienkov, J. Phys. A **27**, L381 (1994).
[9] S.S. Manna, Physica A **187**, 373 (1992).
[10] B.B. Mandelbrot, *The Fractal Geometry of Nature* (Freeman, San Francisco, 1983).
[11] S. Manna and H. Hermann, J. Phys. A **24**, L481 (1991).
[12] T. Aste, Phys. Rev. E **53**, 2571 (1996).